Japanese Journal of Applied Physics
Vol. 46, No. 7A, 2007, pp. 4296–4299

Top-Emitting Organic Light-Emitting Diodes Using Cs/Al/Ag Cathodes

Jong Tae LIM, Chang Hyun JEONG, Mi Suk KIM, June Hee LEE,
Jung Woon BAE, and Geun Young YEOM*

School of Advanced Materials Science and Engineering, SungKyunKwan University, Suwon 440-746, Korea

(Received October 10, 2006; accepted April 3, 2007; published online July 4, 2007)

A semi-transparent cathode composed of Cs (0.5 nm)/Al (2.0 nm)/Ag (20 nm) at the wavelength of 515 nm exhibited the transmittance of 52% and the reflectance of 46%, respectively. The top-emitting device with the glass/Ag (100 nm)/tin-doped indium oxide (ITO, 125 nm)/4,4′,4″-tris[2-naphthylphenyl-1-phenylamino]triphenylamine (2-TNATA, 30 nm)/4,4′-bis[*N*-(1-napthyl)-*N*-phenyl-amino]-biphenyl (NPB, 15 nm)/tris(8-quinolinolato) aluminum(III) (Alq_3, 55 nm)/Cs (0.5 nm)/Al (2 nm)/Ag (20 nm)/Alq_3 (52 nm) structure showed the maximum luminance of 77,200 cd/m^2. Also, the external quantum efficiency and the power efficiency at about 1,000 cd/m^2 were 1.9% and 2.5 lm/W, respectively. It shows about 2 times higher luminous efficiency, compared to the same device structure having lithium fluoride instead of cesium.
[DOI: 10.1143/JJAP.46.4296]

KEYWORDS: TEOLED, top emission, transparent cathode, cesium, aperture ratio

1. Introduction

Organic light-emitting diode (OLED) devices are being developed actively as one of the best flat panel display (FPD) technologies that are suitable for information-display applications of the next generation. Developing top-emitting (TE) OLED structures coupled with a low temperature polycrystalline silicon (LTPS) thin film transistor (TFT) backplane is one of the most essential key-element techniques in active-matrix (AM) OLED displays. TEOLED can provide not only a higher aperture ratio than the general bottom-emitting (BE) one, but also a higher display image quality because of their geometrical merit allowing a high pixel resolution.[1,2] In addition, TEOLED structure provides merits that can easily add a stack of color filter (CF) or color change medium (CCM) and can easily control the color purity of the light irradiated on the top of structure.

In spite of above merits, to keep the characteristics of the intrinsic top emission, two conflicting requirements of the cathode, that is, high electrical conductivity and high transmittance must be simultaneously satisfied. Therefore, designs and fabrication of transparent-conducting cathode in the visible range and the optimization of the device thickness for light out-coupling is one of the key-technologies for high-efficiency TEOLED.

One approach in improving the light-output efficiency of TEOLED is to use low work function metals such as alkali metals (e.g., Li[3,4] and Cs[5,6]) and alkaline earth metals (Mg[7,8] and Ca[9–11]), between an electron-transporting layer (ETL) and an adjoining cathode. Among these metals, work function of cesium is the lowest as 2.14 eV.[12] Various attempts have been made by several research groups to develop new cathode systems such as the semi-transparent conducting buffer layers (STCBLs)/transparent conducting oxides (TCOs) systems (e.g., Ag-doped Mg/tin-doped indium oxide (ITO)[7,8] and Ca/ITO[9]), multi-metal cathode systems (e.g., Ca/Ag,[10] Ca/Mg,[11] and LiF/Al/Ag[12]), and metal-free cathode systems [e.g., CuPc/ITO,[3] Li-doped 2,9-dimethyl-4,7-diphenyl-1,10-phenanthroline (BCP)/tin-doped indium oxide (ITO),[2] and Li-doped 4,7-diphenyl-1,10-phenanthroline (Bphen)/ITO[4]] in recent years. Here, STCBL is generally used to protect organic layers from energetic damages occurring during the deposition of TCO layer.

In this article, we introduce a new Cs/Al/Ag cathode system to TEOLED, to reduce the electron injection barrier from the cathode system into adjoining Alq_3 organic layer. This multilayer cathode is optically transmisive and electrically conductive. Meanwhile, tris(8-quinolinolato) aluminum(III) (Alq_3, refractive index: 1.7[13]) was used as the top capping layer of TEOLED which is a transparent dielectric index-matching layer for the enhancement of optical transmission. The feasibility of the efficient performance of the Alq_3-emitting TEOLED, which is consisted of Cs/Al/Ag cathode, Ag/ITO anode, and Alq_3 refractive index matching layer, will be investigated in the view of optical light-output and luminous efficiency.

2. Experimental Procedure

All the organic layers and metal layers composing the TEOLED were fabricated by vacuum evaporation. Also, ITO composing multilayer anode was fabricated by conventional dc sputtering followed by a heat treatment. The insert of Fig. 1(a) exhibits the schematic diagram of the device structure for Devices 1–3 composed of glass/Ag (100 nm)/ITO (125 nm, about 20–30 Ω/□)/4,4′,4″-tris[2-naphthylphenyl-1-phenylamino]triphenylamine (2-TNATA, 30 nm)/4,4′-bis[*N*-(1-napthyl)-*N*-phenyl-amino]-biphenyl (NPB, 15 nm)/Alq_3 (55 nm)/Cs (x nm)/Al (2.0 nm)/Ag (20 nm)/Alq_3 (52 nm) ($x = 0.5$, 1.0, and 2.0 nm). Device 4 was fabricated as a reference device, which is the same structure except for the 1.0-nm-thick lithium fluoride instead of cesium. Cs (x nm)/Al (2 nm)/Ag (20 nm) and Ag (100 nm)/ITO (125 nm) were used as multilayer cathode and as multilayer anode, respectively. Here, cesium was deposited using a standard SAES getter source. The emissive active area of the devices was 1.4×1.4 mm^2.

The reflectance spectrum and transmittance spectrum of the electrodes were measured by using a ultraviolet–visible–near infrared ray (UV–vis–NIR) spectrophotometer attached with an external DRA (Cary 5000 UV/VIS/NIR, Varian) and a UV spectrophotometer (UV S-2100, SCINCO), respectively. The resistivity was measured by a four-point probe (CMT-SERIES, CHANG MIN). Current–voltage–

*E-mail address: gyyeom@skku.edu

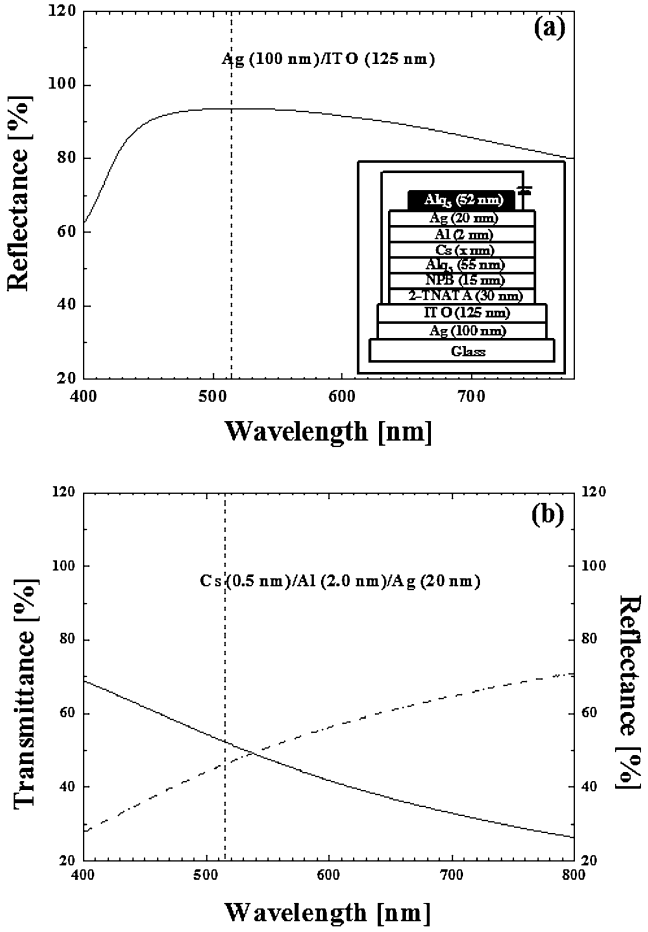

Fig. 1. (a) Reflectance spectrum of the Ag (100 nm)/ITO (125 nm) anode system. The inset is the schematic device structure of the TEOLEDs consisted of glass/Ag (100 nm)/ITO (125 nm)/2-TNATA (30 nm)/NPB (15 nm)/Alq_3 (55 nm)/Cs (x nm)/Al (2.0 nm)/Ag (20 nm)/Alq_3 (52 nm). (b) Transmittance spectrum and reflectance spectrum of the Cs (0.5 nm)/Al (2.0 nm)/Ag (20 nm) cathode system.

luminance characteristics were measured using a source-measure unit (2400, Keithley Instruments), and where, the emission intensity of the OLEDs devices were measured by the photocurrent induced on the silicon photodiodes using a picoammeter (485, Keithley Instruments). Electroluminescent (EL) spectra of the fabricated devices were measured by optical emission spectroscopy (PCM-420, SC Tech.).

3. Results and Discussion

The device configuration of the TEOLED is shown in the insert of Fig. 1(a). Device structure is glass/Ag (100 nm)/ITO (125 nm)/2-TNATA (30 nm)/NPB (15 nm)/Alq_3 (55 nm)/Cs (x nm)/Al (2.0 nm)/Ag (20 nm)/Alq_3 (52 nm). The thickness of cesium for Device 1, Device 2, and Device 3 are 0.5, 1.0, and 2.0 nm, respectively. Among the organic layers, 2-TNATA was used as a hole-injecting layer (HIL), NPB as a hole-transporting layer (HTL), Alq_3 as both a green emissive layer and ETL, respectively.

To achieve the lowest possible operating voltage in TEOLED, it is necessary to have ohmic interfaces between the adjoining organic layer and the charge injecting contacts. In the above TEOLED structure, the ohmic contact to a hole injection layer can be attained when the ionization potential (IP) of 2-TNATA is same as the work function (Φ) of an adjoining anode. Also, the ohmic contact to an electron injection layer can be realized by making the electron affinity (EA) of Alq_3 same as the Φ of an adjoining cathode. In the TEOLED, the energy barrier (ΔH) for a hole injection between ITO (Φ: 4.7 eV)[3] and 2-TNATA (IP: 5.1 eV)[14] is 0.4 eV. However, ΔH for an electron injection between Al (Φ: 4.3 eV) and Alq_3 (EA: 3.1 eV)[15] is about 1.2 eV. Therefore, ΔH for an electron injection is far more high than ΔH for a hole one. Specially, this non-ohmic properties of the above cathode/Alq_3 structure as well as the low mobility of Alq_3, were proved through current–voltage characteristics by Parthasarathy *et al.*[16] Even though ohmic contacts cannot be well formed between the cathode and the organic layers, the injection of an electron carrier into Alq_3 are expected to be improved by introducing cesium between Alq_3 and Al/Ag. Also, the use of cesium with the low Φ of 2.14 eV between an adjoining cathode and Alq_3 is expected to show a good device performance by an efficient electron injection.

Meanwhile, the Ag layer in the Cs/Al/Ag cathode was used as the protecting layer to prevent the oxidation of both Cs and Al sensitive to atmospheric moisture and oxygen. A thin layer of Ag has relatively low optical absorption and the highest conductivity among all metals. The Ag protecting layer is known to improve the lateral electrical conductance of the cathode as reported by Hung *et al.*[13] Also, the Al layer composing the multilayer cathode was inserted to prevent the diffusion of Ag into the Alq_3 layer and to reduce the volatility of Cs for a long time. In addition, Alq_3 (refractive index: 1.7[13]) is used as a dielectric refractive index-matching layer for the enhancement of optical transmission with air (refractive index: 1.0) and as a semi-passivation layer to protect the device.

High reflective mirrors and small cavities are required to achieve a strong radiative emission as the electric field of states is directly proportional to the reflectivity of mirrors and reciprocal of the length of cavity.[17] To obtain a high aperture ratio in this TEOLED study, Ag/ITO is used as a highly reflective anode and Cs/Al/Ag as a highly transmittable cathode with the low resistance. Figure 1(b) shows the transmission and reflectance spectrum as a function of the wavelength over the visible range of multilayer cathode consisted of Cs (0.5 nm)/Al (2.0 nm)/Ag (20 nm). As shown in the figure, the transparency of 52% and the reflectance of 46% could be obtained at the wavelength of 515 nm. The wavelength of 515 nm is the maximum peak of the EL spectrum for Devices 1–3. The high reflectivity of Cs (0.5 nm)/Al (2.0 nm)/Ag (20 nm) is attributed to the silver thickness thicker than the skin depth (δ) of silver. δ of silver can be expressed as follow: $\delta = \lambda/4\pi n_i$ (λ: wavelength, n_i: refractive index). Taking $\lambda = 5 \times 10^{-7}$ m, then $n_i = 3$; consequently, δ is approximately 13 nm.[18] Although the thickness of silver was thicker than the skin depth, the 20-nm-thick silver was applied to the TEOLED in this study for the efficient electrical conduction. Meanwhile, in the visible rage, as the wavelength was decreased, the transmittance of the multilayer cathode composed of Cs (0.5 nm)/Al (2 nm)/Ag (20 nm) was increased while the reflectance was decreased. The multilayer cathode composed of Cs (0.5 nm)/Al (2 nm)/Ag (20 nm) exhibited the resistivity of 8.0×10^{-6} Ω·cm. In the case of the multilayer anode

Table I. Current density–voltage–luminance characteristics of Devices 1–4.

	Thickness of EIL (nm)	η_{ext} (%)	η_{PE} (lm/W)	V_{1000} (V)	V_T (V)	L_{max} (cd/m^2)
Device 1	0.5 (Cs)	1.9	2.5	6.6	2.8	77,200 (11.2 V)
Device 2	1.0 (Cs)	1.3	1.7	6.8	2.8	59,000 (11.6 V)
Device 3	2.0 (Cs)	1.1	1.5	6.8	2.8	49,300 (11.6 V)
Device 4	1.0 (LiF)	1.1	1.2	8.4	3.0	42,600 (12.8 V)

η_{ext}, η_{PE}, and V_{1000} are the values at 1,000 cd/m^2, respectively. V_T and L_{max} are the turn-on voltage at the luminance of 0.1 cd/m^2 and the maximum luminance, respectively.

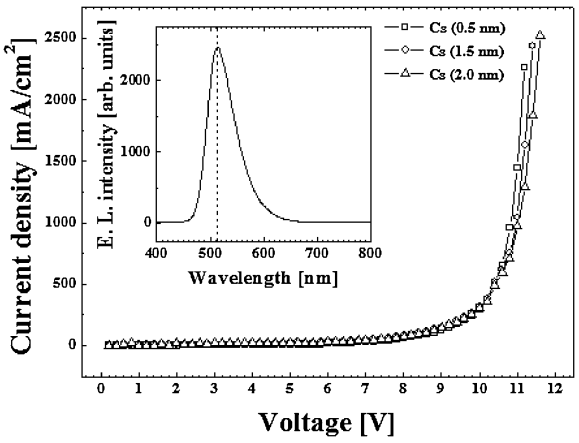

Fig. 2. Current density as a function of the voltage for Devices 1–3. The thickness of the cesium metal in Device 1 (square), Device 2 (circle), and Device 3 (triangle) are 0.5, 1.0, and 2.0 nm, respectively. The inset exhibits the electroluminescent spectrum of Device 1 at a luminance of about 1,000 cd/m^2, corresponding to the forward bias voltage of 6.6 V.

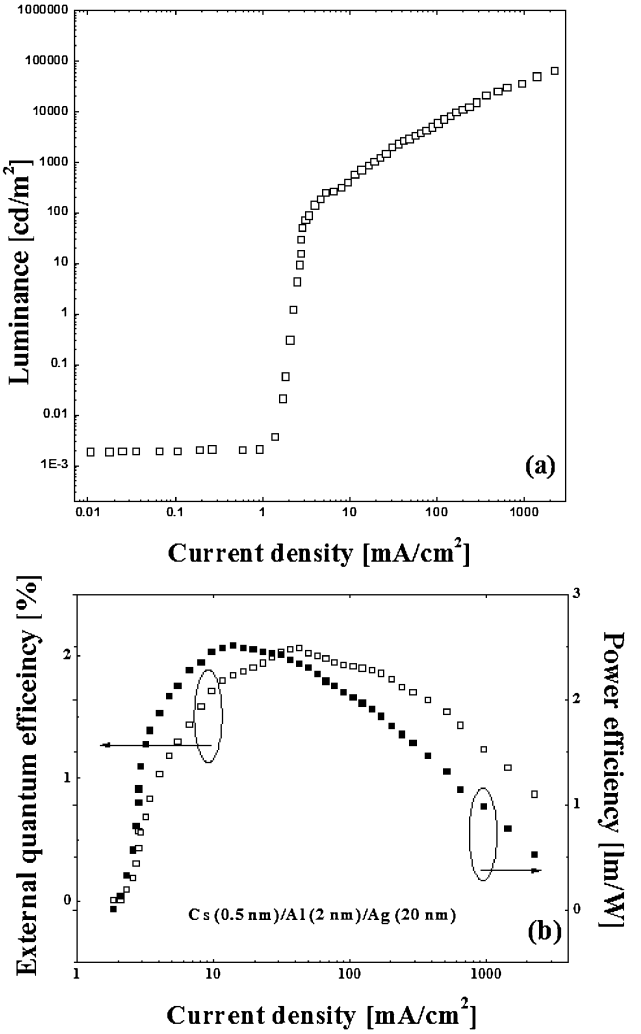

Fig. 3. (a) Luminance as a function of the current density for Device 1. (b) The External quantum efficiency–current density characteristics (open square) and the power efficiency–current density characteristics (closed square) of Device 1.

composed of Ag (100 nm)/ITO (125 nm), the reflectance of 94% could be obtained as shown in Fig. 1(a). The multilayer anode used showed the resistivity of 4.0×10^{-6} Ω·cm.

Figure 2 shows the current density as a function of the forward bias voltage for Devices 1–3. Table I exhibits the current density–voltage–luminance characteristics for Devices 1–4. At the luminance of about 1,000 cd/m^2 (L_{1000}), the current densities of Devices 1–3 were 19.6 (6.6 V), 37.8 (6.8 V), and 42.5 mA/cm^2 (6.8 V), respectively. Voltages of Devices 1–3 at L_{1000} were almost similar as shown in Table I. Device 1 with 0.5-nm-thick cesium is expected to retain the highest power efficiency (η_{PE}) at L_{1000} because the power (W) is inversely proportional to η_{PE} at the same pixel area by the general equation of $\eta_{PE} = \pi \cdot L/J \cdot V$ (J: current density, V: bias voltage). This result is in accord with the relation between the power efficiency and current density for Devices 1–3 shown in Table I.

The inset of Fig. 2 shows the EL spectrum for Device 1 measured at the normal viewing angle and at L_{1000}. As shown in the inset of Fig. 2, the maximum peak of the EL was found at the wavelength of 515 nm. The EL spectrum of 515 nm was tuned by adjusting the macrocavity length,[17] that is, controlled by changing the thickness of ITO composing the multilayer anode.

The maximum luminances (L_{max}) for Devices 1–3 were 77200, 59000, and 49300 cd/m^2, respectively, as shown in Table I. Device 1 with 0.5-nm-thick cesium showed the highest luminance. It is estimated as the results of an efficient electron injection due to the low energy barrier interface between cesium and adjoining Alq_3. On the other hand, Device 4 exhibited lower light-output characteristic than Devices 1–3. Figure 3(a) shows the luminance–current density characteristic for Device 1. In the figure, a sudden change of current density under 3 mA/cm^2 is observed possibly due to the small leakage current of the device. It is believed that this leak current originates from the ITO surface roughness of the device even though more investigation is needed.

Meanwhile, as shown in Devices 1–3 of Fig. 3(a), as the thickness of cesium increases, the luminance of those devices decreases. This phenomenon could be explained by analyzing the electronic structures between Alq_3 and the adjoining cathode as investigated by Lai *et al.*[5] Although the electronic features between Alq_3 and the multilayer cathode used were not investigated, a height of energy barrier fro electron injection from the multilayer cathode

into Alq_3 believes to be the most lowest when the thickness of cesium is 0.5 nm.

The external quantum efficiencies (η_{ext}) at L_{1000} for Devices 1–3 are 1.9, 1.3, and 1.1%, respectively. η_{PE} for Devices 1–3 are 2.5, 1.7, and 1.5 lm/W, respectively. Therefore, Device 1 showed not only the highest η_{PE} but also the highest η_{ext}. The luminous efficiencies in the case of Device 4 exhibited η_{PE} of 1.2 lm/W and η_{ext} of 1.1%, respectively. Therefore, the TEOLED with the Cs/Al/Ag cathode used in this study showed more excellent light output characteristics than that with the LiF/Al/Ag cathode through overall current density–voltage–luminance data.

4. Conclusions

Conventional TEOLED having the Cs/Al/Ag cathode were successfully fabricated by the sequential deposition, in which the structure was consisted of glass/Ag (100 nm)/ITO (125 nm)/2-TNATA (30 nm)/NPB (15 nm)/Alq_3 (55 nm)/Cs (x nm)/Al (2 nm)/Ag (20 nm)/Alq_3 (52 nm). A multilayer cathode composed of Cs (0.5 nm)/Al (2.0 nm)/Ag (20 nm) showed the transmittance of about 52% and the reflectance of about 46%, respectively, at the wavelength of 515 nm. When the thickness of cesium in TEOLED was changed, TEOELD with the 0.5-nm-thick cesium showed the most excellent driving performance in the view of both luminous efficiency and luminance. The light-output of this TEOELD exhibited the L_{max} of 77,200 cd/m^2 at the current density of 2.3 A/m^2 (the forward bias voltage of 11.2 V). Also, its η_{ext} and η_{PE} at L_{1000} (about 6.6 V) were 1.9% and 2.5 lm/W, respectively. This excellent performance was estimated to be possible due to the small energy barrier, which is involved with the efficient electron injection at the interface between cesium with a low Φ and Alq_3. Meanwhile, TEOLEDs having cesium showed about two times higher light out-coupling efficiency, compared to TEOLED of the same structure having LiF instead of Cs. Specially, devices using cesium showed the good driving performance at the low current range before the trapped charge limit current. Although device performance of the Cs/Al/Ag cathode was more excellent than that of the LiF/Al/Ag cathode in TEOLED, it requires an interface investigation between Alq_3 and the Cs/Al/Ag system with the thickness of Ag within the skin depth to improve the optical properties further.

Acknowledgments

This work was supported by the National Research Laboratory Program (NRL) of the Ministry of Science and Technology, and by SungKyunKwan University (2005).

1) G. Gu, G. Parthasarathy, P. Tian, P. E. Burrows, and S. R. Forrest: J. Appl. Phys. **86** (1999) 4076.
2) G. Parthasarathy, C. Adachi, P. E. Burrows, and S. R. Forrest: Appl. Phys. Lett. **76** (2000) 2128.
3) G. Parthasarathy, P. E. Burrows, V. Khalfin, V. G. Kozlov, and S. R. Forrest: Appl. Phys. Lett. **72** (1998) 2138.
4) H. Kanno, Y. Sun, and S. R. Forrest: Appl. Phys. Lett. **86** (2005) 263502.
5) S. L. Lai, M. K. Fung, S. N. Bao, S. W. Tong, M. Y. Chan, C. S. Lee, and S. T. Lee: Chem. Phys. Lett. **367** (2003) 753.
6) G. He, O. Schneider, D. Qin, X. Zhou, M. Pfeiffer, and K. Leo: J. Appl. Phys. **95** (2004) 5773.
7) V. Bulovic, G. Gu, P. E. Burrows, S. R. Forrest, and M. E. Thompson: Nature (London) **380** (1996) 29.
8) G. Gu, V. Bulovic, P. E. Burrows, S. R. Forrest, and M. E. Thompson: Appl. Phys. Lett. **68** (1996) 2606.
9) M.-H. Lu, M. S. Weaver, T. X. Zhou, M. Rothman, R. C. Kwong, M. Hack, and J. J. Brown: Appl. Phys. Lett. **81** (2002) 3921.
10) R. B. Pode, C. J. Lee, D. G. Moon, and J. I. Han: Appl. Phys. Lett. **84** (2004) 4614.
11) H. Riel, S. Karg, T. Beierlein, W. Rieß, and K. Neyts: J. Appl. Phys. **94** (2003) 5290.
12) W. Benenson, J. W. Harris, H. Stocker, and H. Lutz: *Handbook of Physics* (Springer-Verlag, New York, 2002) p. 1082.
13) L. S. Hung, C. W. Tang, M. G. Mason, P. Raychaudhuri, and J. Madathil: Appl. Phys. Lett. **78** (2001) 544.
14) K. Okumoto and Y. Shirota: J. Lumin. **87–89** (2000) 1171.
15) M. A. Baldo and S. R. Forrest: Phys. Rev. B **62** (2000) 10958.
16) G. Parthasarathy, C. Shen, A. Kahn, and S. R. Forrest: J. Appl. Phys. **89** (2001) 4986.
17) M.-H. Lu and J. C. Sturn: J. Appl. Phys. **91** (2002) 595.
18) M. Scalora, M. J. Bloemer, A. S. Pethel, J. P. Dowling, C. M. Bowden, and A. S. Manka: J. Appl. Phys. **83** (1998) 2377.